THE JOURNAL OF PHYSICAL CHEMISTRY B

Article

pubs.acs.org/JPCB

A Novel Cryo-Reduction Method to Investigate the Molecular Mechanism of Nitric Oxide Synthases

Sophie Bernad,[†,§] Albane Brunel,[‡,§] Pierre Dorlet,[‡] Cécile Sicard-Roselli,*[,†] and Jérôme Santolini*[,‡]

[†]Laboratoire de Chimie Physique, CNRS UMR 8000, Univ Paris-Sud, 91405 Orsay Cedex, France

[‡]CNRS, Laboratoire Stress Oxydant et Détoxication, UMR 8221, 91191 Gif-sur-Yvette, France, and CEA, iBiTec-S, SB2SM, 91191 Gif-sur-Yvette, France

Supporting Information

ABSTRACT: Nitric oxide synthases (NOSs) are hemoproteins responsible for the biosynthesis of NO in mammals. They catalyze two successive oxidation reactions. The mechanism of oxygen activation is based on the transfer of two electrons and two protons. Despite structural analogies with cytochromes P450, the molecular mechanism of NOS remains yet to be elucidated. Because of extremely high reaction rates, conventional kinetics methods failed to trap and characterize the major reaction intermediates. Cryo-reduction methods offer a possibility to circumvent this technological lock, by triggering oxygen activation at cryogenic temperatures by using water radiolysis. However, this method is not adapted to the NOS mechanism because of the high instability of the initial $Fe^{II}O_2$ complex (extremely fast autoxidation and/or reaction with the cofactor H_4B). This imposed a protocol with a stable $Fe^{II}O_2$ complex (observed only for one NOS-like protein) and that excludes any redox role for H_4B. A relevant approach to the NOS mechanism would use H_4B to provide the (second) electron involved in oxygen activation; water radiolysis would thus provide the first electron (heme reduction). In this context, we report here an investigation of the first electron transfer by this alternative approach, i.e., the reduction of native NOS by water radiolysis. We combined EPR and resonance Raman spectroscopies to analyze NOS reduction for a combination of different substrates, cofactor, and oxygen concentrations, and for different NOS isoforms. Our results show that cryo-reduction of native NOS is achieved for all conditions that are relevant to the investigation of the NOS mechanism.

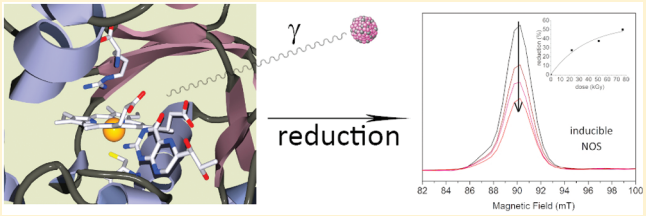

INTRODUCTION

Nitric oxide (NO) is a biological messenger that is involved in numerous physiological events ranging from signaling processes (regulation of vascular tone, neural communication[1,2]) to cytotoxic activities (immune response, tumoricidal agent[3]). In mammals, NO is exclusively synthesized by a family of enzymes named NO-synthases (NOS).[4−6] Because of their involvement in several pathological conditions, NOSs have been the target of numerous biomedical and pharmaceutical investigations. This led to significant progress in the characterization of NOS structure, function, and mechanism.[7−9]

Nitric oxide synthases (NOSs) are hemoproteins that comprise a reductase and an oxygenase domain (Scheme 1). The latter catalyzes a two-step oxidation of a unique substrate, L-arginine (Arg), with formation of N^{ω}-hydroxy-L-arginine (NOHA) as an intermediate.[10] The mechanism of oxygen activation by NOS has long been considered similar to that of cytochromes P450.[11,12] However, in the past decade, several pieces of information suggested that the molecular mechanisms of NOS and P450 are significantly different.[13,14] Indeed, NOS utilizes the crucial cofactor (6*R*)-5,6,7,8-tetrahydro-L-biopterin (H_4B) as an additional source of electrons.[15−17] The potential proton donors are also different and consist of the substrate (Arg), the cofactor (H_4B), or a water molecule.[18−20] Besides, the two NOSs' catalytic steps are based on distinct proton and electron transfer processes.[13,21,22] All recent data support a model that is specific to NOS (Scheme 2): at first, the native ferric heme (**1**) is reduced by the reductase domain into a ferrous species (**2**) that will rapidly bind the dioxygen ligand. The resulting ferrous-oxy species (**3**) will be reduced by H_4B into a ferric-peroxo intermediate (**4**). In the first step (Arg hydroxylation), it is assumed that two successive protonation steps of the distal oxygen atom will favor the heterolytic cleavage of the peroxo O−O bond and the formation of a Compound I-like intermediate (**6**). This intermediate will achieve Arg mono-oxygenation *via* a radical rebound reaction. In the second step (NOHA oxidation), the ferric peroxo intermediate is believed to directly react with the NOHA guanidinium moiety and to lead after a sophisticated electron transfer sequence to H_4B regeneration and NO release (Scheme 2). This model stresses the central role of proton and electron transfers in each catalytic step. Thus, the absence of a clear understanding of these processes has led to the multiplication of diverse (and often opposite) models for the NOS molecular mechanism.[13,14,23−25] The major reason for this is the absence of identification of NOS reaction

Received: January 23, 2012
Revised: April 24, 2012
Published: April 24, 2012

Scheme 1. Structure of the Active Site of the NOS Oxygenase Domain[a]

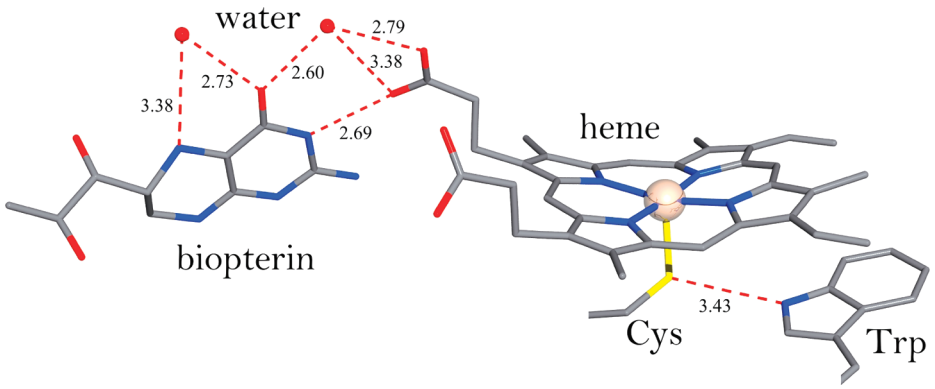

[a]The heme is coordinated by a cysteine residue which is hydrogen-bonded to a tryptophan. The biopterin cofactor is engaged in a hydrogen-bond network with water molecules and one of the heme propionate groups (it is also in hydrogen-bond contact with other aminoacid residues not shown). The figure was generated by using the structure PDB: 2G6M.

Scheme 2. Current Model for the NOS Molecular Mechanism of Oxygen Activation

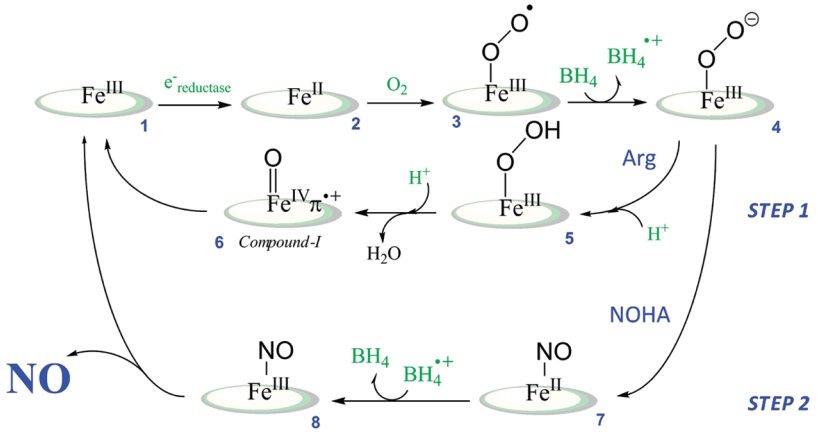

intermediates. This is mostly due to the instability of the initial $Fe^{II}O_2$ complex, which precludes the trapping and characterization of any downstream intermediate by conventional kinetic approaches.[15,26] This constitutes a technological lock to the understanding of the NOS mechanism that calls for a new methodological approach.

Up to now, only Cryo-reduction approaches have allowed the trapping of a peroxo-intermediate.[27−29] This technique analyses the catalytic mechanism in cryogenic conditions. The reaction is triggered by water radiolysis and proceeds by temperature annealing; the reaction intermediates are then identified by EPR spectroscopy.[30,31] If this method gives access to short-lived intermediates, it requires a stable initial $Fe^{II}O_2$ complex. For NOS, it has been obtained only twice, in the absence of H_4B[32] or for a bacterial NOS-like protein.[33] Both experiments imposed conditions that modified the proton and electron processes (no redox cofactor, different distal H-bond network). Thus, the obtained reaction sequence might not reflect the actual molecular mechanism of mammalian NOS. In order to match as closely as possible the natural catalytic cycle, the cryo-reduction protocol must include H_4B as the second electron donor. In these conditions, water radiolysis should provide the first catalytic electron (NOS heme reduction). This approach imposes the use of native ferric enzyme as the initial species in the presence of all required cofactors.

In this work, we report for the first time the use of water radiolysis to achieve the first electron transfer of the NOS mechanism. We combined EPR and resonance Raman spectroscopies to analyze the profile of heme reduction. We analyzed the influence of substrate, cofactor, and oxygen on the reduction yields. We carried out a comparative approach between two different NOSs: iNOS, for which most of the results concerning the mechanism have been obtained, and bsNOS, a bacterial NOS-like protein that is often used as a mimic of mammalian NOSs. Our results show that cryo-reduction of native NOS is achieved for all conditions that are relevant to the investigation of the NOS mechanism.

MATERIAL AND METHODS

Enzyme Preparation. Mouse iNOSoxy and bsNOS recombinant protein were expressed and purified (in the absence or in the presence of H_4B and/or Arg) as described previously.[34−36] Samples were incubated in 100 mM KPi buffer (pH 7.4) in the presence of different combinations of Arg (5 mM) and/or H_4B (800 μM) and washed by two successive dilution−centrifugation cycles in the buffer using CentriCon membrane concentrators with a 30 kDa cutoff (Millipore, Bedford, MA). The samples were then diluted to an enzyme concentration of 200 μM with freshly prepared buffer containing 100 mM potassium phosphate and 20−50% glycerol (v/v) plus Arg (5 mM) and/or H_4B (400 μM). Arg and H_4B

dx.doi.org/10.1021/jp300749b | J. Phys. Chem. B 2012, 116, 5595−5603

binding were verified by UV−visible absorption spectroscopy via the spectral changes of the Soret absorption band from 417 nm (low spin, LS) to 395 nm (high spin, HS). iNOS concentrations were estimated using 71 $mM^{-1}\cdot cm^{-1}$ as an extinction coefficient at 395 nm.[37] Samples (ca. 100 μL) were stored in EPR tubes at 77 K for further use.

Anaerobic ferric iNOSoxy was prepared directly in quartz EPR tubes sealed with airtight rubber septa by 30 cycles of alternate vacuum and argon refilling at room temperature. Ferrous samples were obtained by reduction of Fe^{III} iNOSoxy with the addition of a small volume of dithionite solution (5−10 mM) directly into the EPR tube using a gastight syringe (Hamilton, Reno, NV).

Resonance Raman Spectroscopy. Resonance Raman spectra were recorded at 15 K using a modified single-stage spectrometer (Jobin-Yvon T64000, Jobin-Yvon, Longjumeau, France) equipped with an optical Oxford Instrument Cryostat and a liquid-N_2-cooled back-thinned CCD detector. Stray scattered light was rejected using a holographic notch filter (Kaiser Optical Systems, Ann Arbor, MI). Raman excitation at 413.1 nm was provided by a krypton ion laser (Spectra-Physics 2000, Spectra-Physics, Mountain View, CA).

Spectra were recorded as the coaddition of 40−240 individual spectra with CCD exposure times of 50−100 s each. Three to eight successive sets of such spectra were then averaged. The laser power at the sample was <5 mW. The spectral resolution was 3 cm^{-1}. Baseline correction was performed using GRAMS 32 (Galactic Industries, Salem, NH).

EPR Measurements. CW-EPR spectra were recorded at liquid helium temperatures on a Bruker Elexsys E500 CW-EPR spectrometer equipped with a standard ER 4102 X-band resonator and a continuous flow cryostat (Oxford Instruments). Quantification of the reduction of the pentacoordinated high spin (5cHS) Fe^{III} of the various NOS proteins was achieved by determining the area of the low field peak (around 90 mT) of the EPR signal.

Gamma Radiolysis Experiments. The samples were reduced at 77 K by gamma-irradiation with a panoramic ^{60}Co source (IL 60PL Cis-Bio International) from 16 h up to 50 h with a dose rate of 20−30 Gy/min (determined with a Fricke dosimeter), leading to a total dose from 24 000 Gy up to 76 500 Gy.[38] They were then stored at 77 K until further analysis by EPR and resonance Raman spectroscopies.

RESULTS

Cryo-Reduction of NO-Synthase in the Presence of L-Arginine and H_4B in Anaerobic Conditions. We used cryo-radiolysis to investigate the NOS mechanism of oxygen activation. Native iNOSoxy was irradiated with a panoramic ^{60}Co source for 16 h at 77 K under a nitrogen atmosphere in the presence of saturating concentrations of L-Arg and H_4B. The total irradiation dose was 36.2 kGy. The resonance Raman spectra of the protein, before and after irradiation, and reduced by sodium dithionite, are presented in Figure 1. The high frequency region of the iNOSoxy RR spectrum before irradiation (Figure 1, blue spectrum) is dominated by the vibrational modes ν_4 (1374.2 cm^{-1}), ν_3 (1489.3 cm^{-1}), ν_2 (1562.9 cm^{-1}), ν_{10} (1627.4 cm^{-1}), and ν_5 (1121.6 cm^{-1}) (Supporting Information, Table S1). Those modes are in plane symmetric stretching vibrations involving porphyrin ring carbon or nitrogen atoms[39−41] and provide information about the oxidation, spin, and coordination states of the heme iron. In the low frequency region, the ν_7 and ν_{16} marker bands that

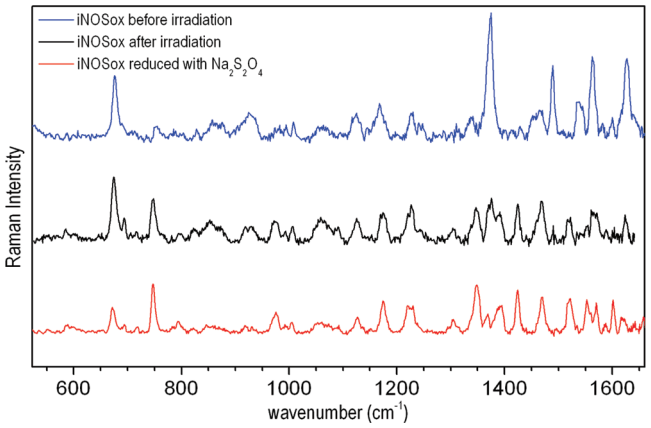

Figure 1. Reduction of NOS proteins upon gamma-irradiation. Resonance Raman spectra of iNOSoxy before irradiation (blue), after irradiation (black), and upon reduction of sodium dithionite (red) in the presence of saturating concentrations of substrate ([L-Arg] = 5 mM) and cofactor ([H_4B] = 400 μM) and in anaerobic conditions (λ_{exc} = 413.1 nm, see the Materials and Methods).

represent in plane porphyrin ring deformation vibrations are observed at 676.9 and 753.9 cm^{-1}, respectively (Supporting Information, Table S1). These frequencies clearly confirm that, in the presence of substrate and cofactor, iNOS heme is in an oxidized five-coordinated high spin state (5cHS), with Cys194 as the proximal ligand.[42]

After irradiation, several changes appear in the RR spectrum of iNOSoxy (Figure 1, black spectrum) that we analyzed in regards to the RR spectrum of a dithionite-reduced iNOSoxy sample (Figure 1, red spectrum): in the high frequency region, the intensity of the ν_4 marker band characteristic of the oxidized species at 1374 cm^{-1} diminishes to the benefit of a ν_4 marker band at 1348 cm^{-1} characteristic of the reduced species, that is also observed through the appearance of some depolarized bands of the ν_4 mode at 1391.9 and 1426.2 cm^{-1}.[43,44] The ν_3 marker band downshifts from 1489 to 1469 cm^{-1}, which is typical for a reduced 5cHS species.[45] In the low frequency region, the ν_{16} mode frequency band downshifts to 747.6 cm^{-1} and its intensity increases significantly. Hence, the RR spectrum of the cryoreduced iNOSoxy contains new contributions similar to those found in the RR spectrum of the iNOS reduced with sodium dithionite (Figure 1, Table S1 in the Supporting Information), indicating the efficiency of cryogenic water radiolysis to reduce Fe^{III} into Fe^{II}. Calculating the intensity bands ratio $I(\nu_{4pp})/I(\nu_7)$ from the RR spectra, we estimated the reduction rate of iNOSoxy in the sample to 35%.

Resonance Raman spectra exhibit bands attributed to the heme being then directly informative of the redox and coordination state of the catalytic site of iNOS. Hence, it could give virtually access to all reaction intermediates. However, RR spectroscopy necessitates lengthy accumulations which did not allow us to repeat several times each experiment to obtain a more precise quantification. Thus, to confirm cryoreduction of iNOSoxy and to improve quantification, EPR spectroscopy was used. EPR, which detects molecules with unpaired electrons, is a method of choice to probe the ferric heme of iNOSoxy. The combined analysis of cryo-reduced samples by EPR and RR is complementary and allows a better identification of the nature and proportion of paramagnetic reaction intermediates, the characterization of their structural and electronic properties.

dx.doi.org/10.1021/jp300749b | J. Phys. Chem. B 2012, 116, 5595−5603

The EPR spectra, recorded at 15 K, of the native and cryo-reduced iNOSoxy in the presence of substrate L-Arg and cofactor H_4B are presented in Figure 2. The iNOSoxy EPR

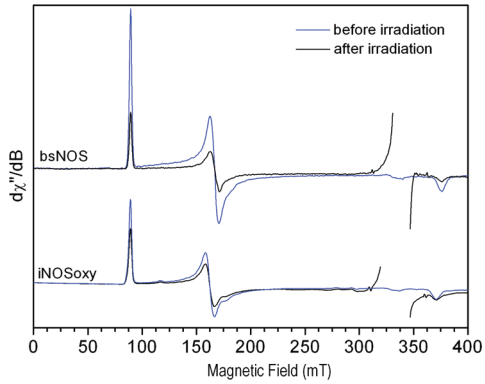

Figure 2. Effect of gamma-irradiation on NOS EPR fingerprints. EPR spectra of iNOSoxy and bsNOS in the presence of saturating concentrations of substrate ([L-Arg] = 5 mM) and cofactor ([H_4B] = 400 μM) before irradiation (blue line) and after irradiation (black line). Experimental conditions were similar as in Figure 1. EPR spectrum conditions were as follows for iNOS after 36.2 kGy: microwave frequency, 9.42 GHz; microwave power, 2 mW; field modulation amplitude, 2.5 mT; temperature, 10 K. For bsNOS after 76.5 kGy: microwave frequency, 9.49 GHz; microwave power, 4.0 mW; field modulation amplitude, 1 mT; temperature, 10 K.

spectrum before irradiation shows a major signal with effective g-values: g_{1eff} = 7.54, g_{2eff} = 4.14, and g_{3eff} = 1.82 (Table S2, Supporting Information). This signal is characteristic of the ferric high spin state species L-Arg-bound NOS in the presence of H_4B.[46] The iron atom in the active site of the protein is pentacoordinated with a proximal cystein ligand. A very minor contribution of a low spin species is also present at g_1 = 2.42, g_2 = 2.28, and g_3 = 1.91. It could be attributed to a six-coordinated bisthiolate species.[46] After irradiation, the HS state species signal of iNOSoxy decreases. By calculating the ratio of the g_{1eff} signal intensity after and before irradiation, we obtain 34% of reduction (Figure 2, bottom). This confirms the ability to achieve native iNOS reduction by water radiolysis in cryogenic conditions in the presence of both substrate and cofactor. The yields of reduction obtained by EPR and RR spectroscopies are in good agreement. Hence, for all irradiation experiments, we calculated the reduction rate from the EPR spectra.

Effect of Substrate, Cofactor, and Oxygen on the Reduction Rate. We studied the effect of the irradiation dose on the reduction yield. Figure 3A represents the reduction rate of iNOSoxy in anaerobic conditions with Arg/H_4B as a function of the irradiation dose. The reduction yield seems to increase until reaching a plateau around 50−60%, which is close to what has been reported on myoglobin (around 75%[47]). Differences with the myoglobin reduction could be due to protein specificity, to the glycerol percentage (50% glycerol in our samples instead of 65% glycerol[47]), or to differences in the dose rate (between 20 and 30 Gy/min in our case instead of 200 Gy/min for Denisov[47]).

We analyzed the extent of iNOSoxy reduction as a function of the irradiation dose for different conditions. Figure 3B shows the progressive disappearance of ferric iNOSoxy in the presence of saturating concentrations of H_4B. The inset shows the yield of reduction as a function of the irradiation dose, with a final reduction yield around 60%. The same experiment has been achieved for various combinations of substrate (L-Arg or NOHA) and cofactor. We observed a similar disappearance of native iNOSoxy as a function of the irradiation dose (data not shown). The final reduction yield (at 76.5 kGy) ranges between 50 and 74% (see Table 1). This result suggests that the presence of substrates and cofactor does not dramatically interfere with the water radiolysis and the reduction of NOS heme. We also analyzed the effect of the presence of oxygen on the cryo-reduction process. Figure 3 displays the progressive reduction of iNOSoxy in air-saturated conditions in the presence of H_4B (Figure 3D) and both H_4B and L-Arg (Figure 3C). We repeated the same experiment for all combinations of L-Arg and H_4B (data not shown). We observed the same reduction yield (within 10% margin) in the presence or in the absence of dioxygen (Table 1). This suggests that dioxygen does not significantly prevent heme reduction by reacting with solvated electron.

Cryo-Reduction of a Bacterial NOS-like Protein, bsNOS. Bacterial NOS-like proteins have been used as a model in particular for cryo-assays where the reports on NOS from *Geobacillus stearothermophilus* are central.[33] We therefore checked the structural integrity upon the cryoreduction procedure of another bacterial NOS-like protein from *Bacillus subtilis*, bsNOS. bsNOS was gamma-irradiated under the same conditions (77 K, 50% glycerol buffer, 76.5 kGy) in the presence of L-Arg and H_4B. We recorded the resonance Raman spectrum of bsNOS after irradiation (data not shown). We observed the appearance of similar bands characteristic of ferrous heme species. The frequencies of the major porphyrin modes (ν_2 at 1572 cm^{-1}, ν_3 at 1467 cm^{-1}, ν_4 at 1348 cm^{-1}, ν_7 at 677 cm^{-1}, ν_{10} at 1602 cm^{-1}, ν_{16} at 748 cm^{-1}) are similar to those we previously reported for ferrous bacterial NOSs in standard conditions.[43,48] This suggests that, like iNOSoxy, bsNOS is reduced upon water radiolysis. This result was also confirmed by EPR analysis. As for iNOSoxy, the EPR spectrum of bsNOS before irradiation exhibits three effective g-values—g_{1eff} = 7.59, g_{2eff} = 4.07, and g_{3eff} = 1.80 (Figure 2, Table S2 in the Supporting Information)—that are characteristic of a ferric high spin state.[49] Similar to what we observed for iNOSoxy, gamma-irradiation induces a disappearance of the HS state signal of bsNOS (Figure 2, top). We also analyzed the effect of the presence of substrate, cofactor, and dioxygen on the cryo-reduction process of bsNOS. Figure 4 displays the dose−response of bsNOS reduction upon gamma-irradiation for six different combinations of substrate (NOHA or L-Arg) and cofactor (H_4B) in air-saturated conditions. The reduction yields (at 76.5 kGy) ranged between 28 and 67% for all the conditions we tested. We repeated the same experiment in the absence of dioxygen (data not shown). We did not see a significant effect of the presence of dioxygen on the reduction yield for all the conditions we tested (Table 1).

In summary, the results obtained for bsNOS are identical to those obtained for iNOSoxy. It appears that the nature of the NOS protein has only a marginal effect on the cryo-reduction yield. *In fine*, of the 21 different conditions we investigated, around 75% display percentage yields between 50 and 70% for a 76.5 kGy irradiation (Table 1). Given the fact that a great number of conditions were tested, it was not possible to replicate several times all the assays. Therefore, we estimate that the differences observed on some samples are within experimental error and not significant considering the experimental setup (small changes in irradiation doses, concentrations, annealing, etc.). This suggests that the presence

dx.doi.org/10.1021/jp300749b | J. Phys. Chem. B 2012, 116, 5595−5603

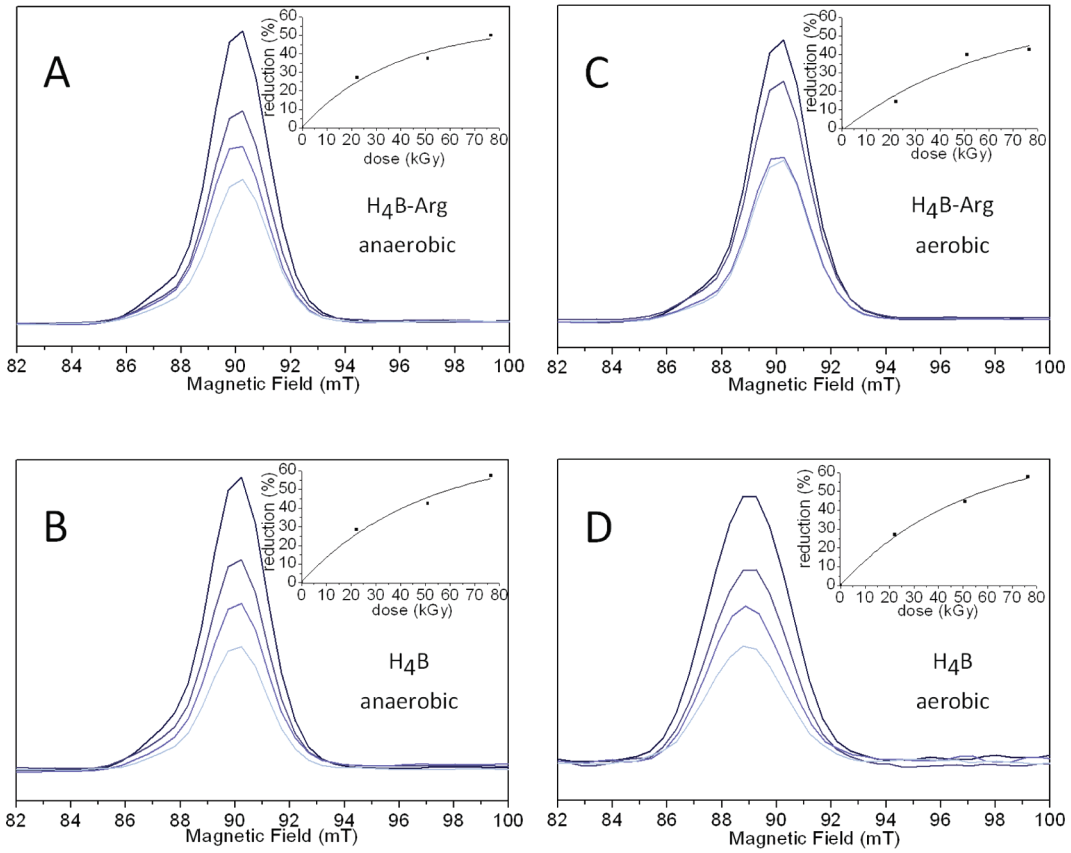

Figure 3. Dose−response of iNOSoxy reduction upon gamma-irradiation. Experimental conditions as described under the Materials and Methods. EPR spectrum conditions were as follows: microwave frequency, 9.42 GHz; microwave power, 2 mW; field modulation amplitude, 2.5 mT; temperature, 10 K. Panel A: g_{1eff} EPR signal of ferric iNOSoxy in the presence of saturating concentrations of substrate ([L-Arg] = 5 mM) and cofactor ([H_4B] = 400 μM) for increasing irradiation doses (before irradiation and after 22.2, 51, and 76.5 kGy). Inset: reduction yield as a function of the irradiation dose. Panel B: same as in panel A but in the absence of L-Arg. Panels C and D: same as in panels A and B, respectively, but in air-saturated conditions.

of Arg, H_4B, or oxygen does not drastically interfere with the NOS cryo-reduction process. Our results also suggest that dioxygen does not significantly interfere with the capture by NOS of solvated electrons, which would lessen NOS reduction.

DISCUSSION

Conservation of NOS Heme Structure under Cryo-Assays Conditions. The cryo-reduction setup requires extreme experimental conditions: NOS samples are stored in liquid nitrogen at 77 K, exposed to high doses of γ-rays, and then analyzed at temperatures around 10 K. We used a glycerol/buffer mixture as a standard cryoprotectant that has been commonly used to study proteins such as hemoglobin, heme oxygenase, cytochrome P450, or peroxidase.[27,50−54] Since the central steps of the NOS molecular mechanism—electron and proton transfers—are extremely sensitive to the structure of the catalytic site and thus to the milieu conditions, it is mandatory to check that these extreme experimental conditions do not affect the structure and the function of the enzyme.

We first analyzed the spin and coordination states of iNOSoxy for our series of substrate (L-Arg and NOHA) and cofactor combination throughout the experimental sequence. They directly inform on NOS quaternary structure and on its ability to carry out L-Arg oxidation. The resonance Raman and EPR spectra of iNOSoxy for each complex indicate the presence of the expected states, i.e., 5cHS in the presence of substrate and/or cofactor and 6cLS in the absence of cofactor and substrate. This indicates that the high concentration of glycerol and the freezing steps do not disturb the 5cHS−6cLS equilibrium, i.e., the iNOSoxy quaternary structure.

We also recorded and compared the resonance Raman spectra of irradiated and non-irradiated iNOSoxy for all the tested conditions. Figure 1 illustrates this comparison for iNOSoxy with L-Arg and H_4B before and after gamma-irradiation (Figure 1). The frequencies of the characteristic vibrational modes of ferric NOS (ν_2, ν_3, ν_4, ν_5, ν_7, ν_{10}, and ν_{16}) are similar and match those previously reported for iNOSoxy in standard conditions; the same observation was made for each of the tested conditions (Supporting Information, Table S1). This indicates the absence of modifications of the iNOSoxy catalytic site related to the production of reactive species that could have reacted with residues or cofactors of the NOS catalytic site. In particular, no oxidation/reduction of porphyrin macrocycle is to be reported. The same experiment has been achieved under air-saturated conditions. Identical frequencies were observed for the porphyrin vibration modes, indicating the absence of additional oxidative reactions in the presence of dioxygen (Supporting Information, Table S1). We achieved the same comparative analysis of cryo-reduced and dithionite-reduced iNOSoxy, in nitrogen- and air-saturated buffers, and for various combinations of substrate and cofactor. Once again, the frequencies that we determined were similar for both ferrous NOS and matched those reported in the literature (ref 45, Supporting Information, Table S1) Similarly, the EPR spectra

dx.doi.org/10.1021/jp300749b | J. Phys. Chem. B 2012, 116, 5595−5603

Table 1. Reduction Yield of iNOSoxy and bsNOS upon Cryo-Reduction (Yields Were Determined from the Decrease of the Low Field Peak of the Ferric EPR Signal)

			reduction yield (%)		
	substrate-cofactor	oxygen conditions	22.2 kGy	51.0 kGy	76.5 kGy
iNOSoxy	Arg and H_4B free	aerobic 20%	19	62	64
		anaerobic	51	64	74
	Arg-H_4B	aerobic 20%	15	40	42
		anaerobic	27	38	50
	Arg	aerobic 20%	17	43	61
		anaerobic	25	Nd	62
	H_4B	aerobic 20%	27	45	58
		anaerobic	29	43	57
	NOHA-H_4B	aerobic 20%	25	49	61
	NOHA	aerobic 20%	15	25	70
bsNOS	Arg and H_4B free	aerobic 20%	17	44	49
		anaerobic	26	Nd	60
	Arg-H_4B	aerobic 20%	23	55	67
		anaerobic	21	47	63
	Arg	aerobic 20%	40	51	60
		anaerobic	22	41	55
	H_4B	aerobic 20%	25	26	33
		anaerobic	20	42	57
	NOHA-H_4B	aerobic 20%	10	19	28
	NOHA	aerobic 20%	9	32	46

of iNOSoxy and bsNOS HS heme exhibit identical *g*-values before and after irradiation (Figure 2, Supporting Information, Table S2), confirming the absence of structural alteration of the catalytic site of bsNOS and iNOSoxy upon gamma-irradiation (this does not exclude potential oxidative modifications of NOS on other locations, for example, on the protein surface).

These results indicate that the whole experimental procedure (high content of glycerol, analysis at cryogenic temperature, high dose of gamma-irradiation, etc.) does not affect the spectroscopic fingerprints (both EPR and resonance Raman) of two different NOS proteins, suggesting a good conservation throughout the cryo-assays of the catalytic site properties.

We also analyzed the impact of the cryo-reduction protocol on the functioning of iNOSoxy for two distinct conditions: with H_4B and with L-Arg. We first recorded the UV−visible absorption spectra of the iNOSoxy $Fe^{II}CO$ complex after supplementation with saturating concentrations of L-Arg and H_4B. The P450/P420 equilibrium reflects the stability of the proximal thiolate ligation, that is essential to NOS catalysis.[55,56] We compared the extent of P420 formation for native, frozen, and irradiated (60 kGy) samples to analyze the degradation of the NOS catalytic site. In the case of the iNOSoxy + H_4B sample, the percentage of pentacoordinated $Fe^{II}CO$ complex (P420) remains negligible (Supporting Information, Figure S1A, inset). In the case of the iNOSoxy + L-Arg sample, the absorption at 420 nm slightly increases (the greater proportion of P420 complex for the +L-Arg sample is due to the weaker ability of the substrate to induce the hexacoordinated low spin, 6cLS → 5cHS transition of iNOSoxy) but remains minor and comparable for the three (native, frozen, irradiated) samples. These results indicate that the freezing and irradiation sequence does not disturb the thiolate binding of iNOSoxy. We also analyzed the effect of the freezing and irradiation procedure on the ability of iNOSoxy to achieve oxygen activation and catalyze substrate oxidation. For this purpose, we used the Griess assay with NOHA as a substrate[57] and monitored the effect of increasing concentration of H_4B on the production of nitrite. For all conditions (+L-Arg or +H_4B), the production of nitrite was comparable to what is commonly expected for iNOSoxy and was affected neither by the freezing nor by the irradiation (Supporting Information, Figure S1, main panels). Additionally, the apparent K_d of H_4B was similar for the three curves and found around 5 μM, close to what is reported in the literature.[58,59] This suggests that the experimental protocol does not affect H_4B binding and thus does not impede its crucial role in NOS catalysis. This series of results show unambiguously and definitely that the protocol used during the cryo-reduction experiments does not alter neither NOS structural and electronic properties, nor its functioning. Our data can therefore be cross-analyzed with results obtained through more conventional methods.

Alternative Radiolysis Technique to Investigate the NOS Molecular Mechanism. Water radiolysis in cryogenic conditions has been successfully used by Davydov and Hoffman to investigate the molecular mechanism of cytochromes P450 and numerous other hemo-proteins.[30] Their approach focuses on the second electron transfer (oxygen activation) and requires the build-up and trapping of a quantitative amount of $Fe^{II}O_2$ complex. However, mammalian NOSs are characterized by a great instability of the $Fe^{II}O_2$ complex especially in the presence of the H_4B cofactor (decay rate up to 25 s^{-1} at 10 °C). This might explain why this method has only been used twice for NOS, first in the absence of H_4B[32] and second for a bacterial NOS-like protein that presents a stable $Fe^{II}O_2$ intermediate[33] (decay rate of 1.4 s^{-1} at room temperature). In this regard, a method that overcomes the obstacle of $Fe^{II}O_2$ instability seems required to investigate the molecular mechanism of mammalian NOS.

Our study lays the path for a new method to investigate the NOS molecular mechanism of dioxygen activation. This alternative method is based on the use of water radiolysis to provide the first electron (heme reduction), while oxygen activation would be triggered by the transfer of a second electron by the natural electron donor, H_4B. We analyzed in this work the efficiency and properties of heme reduction by water radiolysis. To our knowledge, this is the first time such a complete study is achieved for a hemo-protein. In the case of NOS, heme reduction by the reductase domain is a sophisticated process with numerous regulation patterns.[60] The reduction rate varies greatly among NOS isoforms. It depends on the presence of substrate and cofactor, on the presence of dioxygen, on the conformational state of the dimer, etc. We showed in this report that the heme reduction induced by water radiolysis was quantitative for a wide series of conditions: (i) we observed the same (high) reduction yield for distinct NOS isoforms (bsNOS vs iNOSoxy), which *a priori* allows the comparative analysis of isoforms; (ii) we also observed similar reduction yield for various quaternary structures of NOS such as loose dimer (iNOSoxy in the absence of substrate and cofactor,[58,61] tight dimer iNOSoxy in the presence of substrate and cofactor,[12,62] or dimer with an open interface bsNOS[63]); (iii) the reduction profile did not depend on the nature of the substrates or the presence of dioxygen, which allows the comparison of the different catalytic cycles of NOS (first and second steps, NO dioxygenase activity); (iv) the presence of H_4B, that is crucial in the electron and proton transfer processes, does not influence the reduction

dx.doi.org/10.1021/jp300749b | J. Phys. Chem. B 2012, 116, 5595−5603

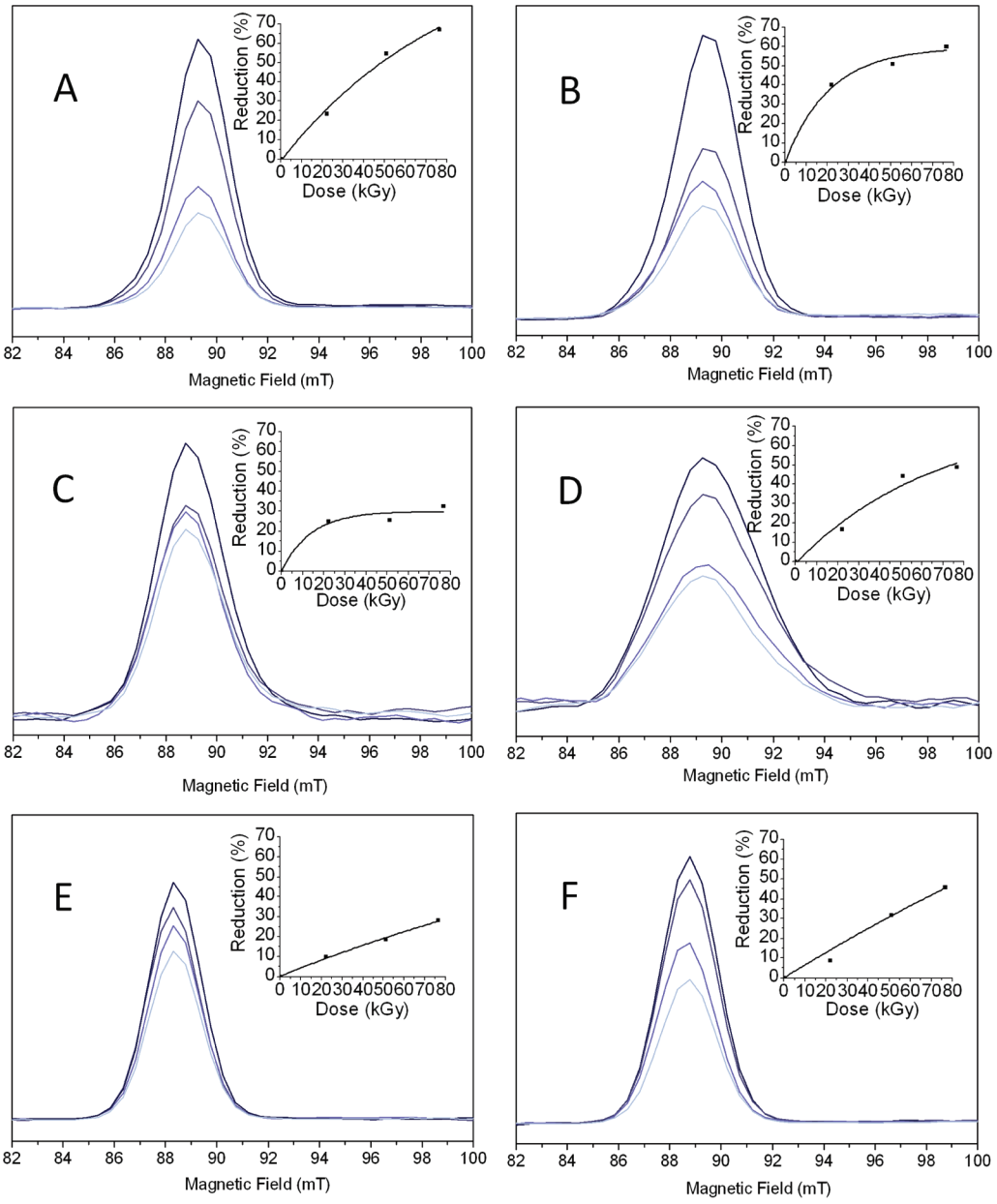

Figure 4. Dose−response of bsNOS reduction upon gamma-irradiation. Experimental conditions as described under the Materials and Methods. EPR spectrum conditions were as follows: microwave frequency, 9.49 GHz; microwave power, 4.0 mW; field modulation amplitude, 1 mT; temperature, 10 K. Panel A: g_1 EPR spectra of ferric bsNOSoxy in the presence of saturating concentrations of substrate ([L-Arg] = 5 mM) and cofactor ([H_4B] = 400 μM) for increasing irradiation doses (before irradiation and after 22.2, 51.0, and 76.5 kGy). Spectra are in gray, and simulations are in black. Inset. Reduction yield as a function of the irradiation dose. Other panels: Same as in panel A but in the absence of H_4B (B), in the absence of L-Arg (C), in the absence of H_4B and L-Arg (D), in the presence of NOHA and H_4B (E), and in the presence of NOHA without H_4B (F).

yield. These results show that this cryo-reduction protocol can be used for a large series of conditions that will allow a complete investigation of NOS catalysis.

Our results show that all NOS proteins can be investigated with the same protocol. This will allow us to directly compare the reaction sequences of mammalian and bacterial NOSs and to highlight potential differences in their molecular mechanism. Thanks to the presence of H_4B, we will analyze the natural electron transfer process and, in this regard, we will detail and explain the differences in the oxidation reaction (nucleophilic attack vs heterolytic cleavage) between the first and second catalytic steps. The presence of H_4B could allow us to specifically analyze the role of H_4B in the proton transfer sequence and to address the question of proton-coupled electron transfer.

CONCLUSION

We report here the first investigation of cryo-reduction of native NOS isoforms for a large series of conditions that include variations in isoforms, substrates, cofactor, and oxygen concentration. During this study, we verified the structural and functional integrity of the NOS catalytic site upon the extreme experimental conditions used during cryo-assays. This will allow correlating unambiguously the reaction sequence observed by the cryo-reduction method to the results previously obtained by

dx.doi.org/10.1021/jp300749b | J. Phys. Chem. B 2012, 116, 5595−5603

more conventional kinetic methods (stopped-flow, freeze-quench, enzymatic assays).

The possibility to compare the oxidation reaction for different isoforms, substrates, and cofactor will provide answers to the specificity of each catalytic step and will allow tracking the differences between the numerous NOS and NOS-like proteins. This new protocol will also give the opportunity to analyze the proton transfer pathways that lie at the core of the NOS molecular mechanism. In particular, this method allows investigating the conditions that favor NOS uncoupling (the absence of substrate and/or cofactor). This should permit the characterization of the molecular mechanism of RNOS production, in particular the precise role of decoupled proton and electron transfers and the specificity of each NOS isoform regarding the uncoupling scenarios.

■ ASSOCIATED CONTENT

Supporting Information

Table S1 showing vibrational modes of the porphyrin of iNOSoxy before and after gamma-irradiation, Table S2 showing *g*-values of the 5cHS species of FeIII of iNOS and bsNOS before and after irradiation, and Figure S1 showing the impact of gamma-irradiation on iNOSoxy structure and function. This material is available free of charge via the Internet at http://pubs.acs.org.

■ AUTHOR INFORMATION

Corresponding Author

*Phone: (33) 1 69 15 77 32 (C.R.-S.); (33) 1 69 08 53 63 (J.S.). Fax: (33) 1 69 15 61 88 (C.R.-S.); (33) 1 69 08 87 17 (J.S.). E-mail: cecile.sicard@u-psud.fr (C.R.-S.); jerome.santolini@cea.fr (J.S.).

Author Contributions

§Both authors contributed equally to this work.

Notes

The authors declare no competing financial interest.

■ REFERENCES

(1) Bredt, D. S. *J. Cell Sci.* **2003**, *116*, 9−15.
(2) Ignarro, L. J. *J. Physiol. Pharmacol.* **2002**, *53*, 503−514.
(3) Bogdan, C. *Nat. Immunol.* **2001**, *2*, 907−916.
(4) Lowenstein, C. J.; Padalko, E. *J. Cell Sci.* **2004**, *117*, 2865−2867.
(5) Mungrue, I. N.; Bredt, D. S. *J. Cell Sci.* **2004**, *117*, 2627−2629.
(6) Sessa, W. C. *J. Cell Sci.* **2004**, *117*, 2427−2429.
(7) Stuehr, D. J.; Santolini, J.; Wang, Z. Q.; Wei, C. C.; Adak, S. *J. Biol. Chem.* **2004**, *279*, 36167−36170.
(8) Alderton, W. K.; Cooper, C. E.; Knowles, R. G. *Biochem. J.* **2001**, *357*, 593−615.
(9) Li, H.; Poulos, T. L. *J. Inorg. Biochem.* **2005**, *99*, 293−305.
(10) Stuehr, D. J.; Kwon, N. S.; Nathan, C. F.; Griffith, O. W.; Feldman, P. L.; Wiseman, J. *J. Biol. Chem.* **1991**, *266*, 6259−6263.
(11) Poulos, T. L. *Biochem. Biophys. Res. Commun.* **2005**, *338*, 337−345.
(12) Crane, B. R.; Arvai, A. S.; Ghosh, D. K.; Wu, C.; Getzoff, E. D.; Stuehr, D. J.; Tainer, J. A. *Science* **1998**, *279*, 2121−2126.
(13) Santolini, J. *J. Inorg. Biochem.* **2011**, *105*, 127−141.
(14) Zhu, Y.; Silverman, R. B. *Biochemistry* **2008**, *47*, 2231−2243.
(15) Hurshman, A. R.; Krebs, C.; Edmondson, D. E.; Huynh, B. H.; Marletta, M. A. *Biochemistry* **1999**, *38*, 15689−15696.
(16) Wei, C. C.; Wang, Z. Q.; Wang, Q.; Meade, A. L.; Hemann, C.; Hille, R.; Stuehr, D. J. *J. Biol. Chem.* **2001**, *276*, 315−319.
(17) Bec, N.; Gorren, A. F. C.; Mayer, B.; Schmidt, P. P.; Andersson, K. K.; Lange, R. *J. Inorg. Biochem.* **2000**, *81*, 207−211.
(18) Li, D.; Kabir, M.; Stuehr, D. J.; Rousseau, D. L.; Yeh, S. R. *J. Am. Chem. Soc.* **2007**, *129*, 6943−6951.
(19) Giroud, C.; Moreau, M.; Mattioli, T. A.; Balland, V.; Boucher, J. L.; Xu-Li, Y.; Stuehr, D. J.; Santolini, J. *J. Biol. Chem.* **2010**, *285*, 7233−7245.
(20) Chartier, F. J.; Couture, M. *J. Biol. Chem.* **2007**, *282*, 20877−20886.
(21) Korth, H. G.; Sustmann, R.; Thater, C.; Butler, A. R.; Ingold, K. U. *J. Biol. Chem.* **1994**, *269*, 17776−17779.
(22) Doukov, T.; Li, H.; Soltis, M.; Poulos, T. L. *Biochemistry* **2009**, *48*, 10246−10254.
(23) Robinet, J. J.; Cho, K. B.; Gauld, J. W. *J. Am. Chem. Soc.* **2008**, *130*, 3328−3334.
(24) de Visser, S. P.; Tan, L. S. *J. Am. Chem. Soc.* **2008**, *130*, 12961−12974.
(25) Cho, K. B.; Carvajal, M. A.; Shaik, S. *J. Phys. Chem. B* **2009**, *113*, 336−346.
(26) Wei, C. C.; Wang, Z. Q.; Durra, D.; Hemann, C.; Hille, R.; Garcin, E. D.; Getzoff, E. D.; Stuehr, D. J. *J. Biol. Chem.* **2005**, *280*, 8929−8935.
(27) Davydov, R.; Makris, T. M.; Kofman, V.; Werst, D. E.; Sligar, S. G.; Hoffman, B. M. *J. Am. Chem. Soc.* **2001**, *123*, 1403−1415.
(28) Davydov, R.; Perera, R.; Jin, S.; Yang, T. C.; Bryson, T. A.; Sono, M.; Dawson, J. H.; Hoffman, B. M. *J. Am. Chem. Soc.* **2005**, *127*, 1403−1413.
(29) Denisov, I. G.; Mak, P. J.; Makris, T. M.; Sligar, S. G.; Kincaid, J. R. *J. Phys. Chem. A* **2008**, *112*, 13172−13179.
(30) Davydov, R.; Hoffman, B. M. *Arch. Biochem. Biophys.* **2011**, *507*, 36−43.
(31) Denisov, I. G.; Makris, T. M.; Sligar, S. G. *Methods Enzymol.* **2002**, *357*, 103−115.
(32) Davydov, R.; Ledbetter-Rogers, A.; Martasek, P.; Larukhin, M.; Sono, M.; Dawson, J. H.; Masters, B. S.; Hoffman, B. M. *Biochemistry* **2002**, *41*, 10375−10381.
(33) Davydov, R.; Sudhamsu, J.; Lees, N. S.; Crane, B. R.; Hoffman, B. M. *J. Am. Chem. Soc.* **2009**, *131*, 14493−14507.
(34) Ghosh, D. K.; Wu, C.; Pitters, E.; Moloney, M.; Werner, E. R.; Mayer, B.; Stuehr, D. J. *Biochemistry* **1997**, *36*, 10609−10619.
(35) Gachhui, R.; Ghosh, D. K.; Wu, C.; Parkinson, J.; Crane, B. R.; Stuehr, D. J. *Biochemistry* **1997**, *36*, 5097−5103.
(36) Adak, S.; Aulak, K. S.; Stuehr, D. J. *J. Biol. Chem.* **2002**, *277*, 16167−16171.
(37) Stuehr, D. J.; Ikedasaito, M. *J. Biol. Chem.* **1992**, *267*, 20547−20550.
(38) Spinks, J. W. T.; Woods, R. J. *An Introduction to Radiation Chemistry*; John Wiley and Sons, Inc.: New York, Toronto, 1990.
(39) Spiro, T. G.; Strekas, T. C. *J. Am. Chem. Soc.* **1974**, *96*, 338−345.
(40) Gaber, B. P.; Miskowski, V.; Spiro, T. G. *J. Am. Chem. Soc.* **1974**, *96*, 6868−6873.
(41) Hu, S. Z.; Morris, I. K.; Singh, J. P.; Smith, K. M.; Spiro, T. G. *J. Am. Chem. Soc.* **1993**, *115*, 12446−12458.
(42) Crane, B. R.; Arvai, A. S.; Gachhui, R.; Wu, C.; Ghosh, D. K.; Getzoff, E. D.; Stuehr, D. J.; Tainer, J. A. *Science* **1997**, *278*, 425−431.
(43) Santolini, J.; Roman, M.; Stuehr, D. J.; Mattioli, T. A. *Biochemistry* **2006**, *45*, 1480−1489.
(44) Wells, A. V.; Li, P.; Champion, P. M.; Martinis, S. A.; Sligar, S. G. *Biochemistry* **1992**, *31*, 4384−4393.
(45) Wang, J.; Stuehr, D. J.; Ikeda-Saito, M.; Rousseau, D. L. *J. Biol. Chem.* **1993**, *268*, 22255−22258.
(46) Salerno, J. C.; Martasek, P.; Roman, L. J.; Masters, B. S. *Biochemistry* **1996**, *35*, 7626−7630.
(47) Sligar, S. G.; Denisov, I. G.; Victoria, D. C. *Radiat. Phys. Chem.* **2007**, *76*, 714−721.
(48) Chartier, F. J.; Couture, M. *Biophys. J.* **2004**, *87*, 1939−1950.
(49) Brunel, A.; Wilson, A.; Henry, L.; Dorlet, P.; Santolini, J. *J. Biol. Chem.* **2011**, *286*, 11997−12005.
(50) Davydov, R.; Osborne, R. L.; Kim, S. H.; Dawson, J. H.; Hoffman, B. M. *Biochemistry* **2008**, *47*, 5147−5155.

(51) Davydov, R.; Osborne, R. L.; Shanmugam, M.; Du, J.; Dawson, J. H.; Hoffman, B. M. *J. Am. Chem. Soc.* **2010**, *132*, 14995−15004.
(52) Davydov, R.; Valentine, A. M.; Komar-Panicucci, S.; Hoffman, B. M.; Lippard, S. J. *Biochemistry* **1999**, *38*, 4188−4197.
(53) Davydov, R.; Kofman, V.; Fujii, H.; Yoshida, T.; Ikeda-Saito, M.; Hoffman, B. M. *J. Am. Chem. Soc.* **2002**, *124*, 1798−1808.
(54) Davydov, R.; Kofman, V.; Nocek, J. M.; Noble, R. W.; Hui, H.; Hoffman, B. M. *Biochemistry* **2004**, *43*, 6330−6338.
(55) Wang, J.; Stuehr, D. J.; Rousseau, D. L. *Biochemistry* **1995**, *34*, 7080−7087.
(56) Martinis, S. A.; Blanke, S. R.; Hager, L. P.; Sligar, S. G.; Hoa, G. H.; Rux, J. J.; Dawson, J. H. *Biochemistry* **1996**, *35*, 14530−14536.
(57) Titheradge, M. A. *Nitric oxide protocols*; Humana Press: Totowa, NJ; 1998.
(58) Presta, A.; Siddhanta, U.; Wu, C.; Sennequier, N.; Huang, L.; Abu-Soud, H. M.; Erzurum, S.; Stuehr, D. J. *Biochemistry* **1998**, *37*, 298−310.
(59) Tzeng, E.; Billiar, T. R.; Robbins, P. D.; Loftus, M.; Stuehr, D. J. *Proc. Natl. Acad. Sci. U.S.A.* **1995**, *92*, 11771−11775.
(60) Stuehr, D. J.; Tejero, J.; Haque, M. M. *FEBS J.* **2009**, *276*, 3959−3974.
(61) Panda, K.; Rosenfeld, R. J.; Ghosh, S.; Meade, A. L.; Getzoff, E. D.; Stuehr, D. J. *J. Biol. Chem.* **2002**, *277*, 31020−31030.
(62) Mayer, B.; Wu, C.; Gorren, A. C.; Pfeiffer, S.; Schmidt, K.; Clark, P.; Stuehr, D. J.; Werner, E. R. *Biochemistry* **1997**, *36*, 8422−8427.
(63) Pant, K.; Bilwes, A. M.; Adak, S.; Stuehr, D. J.; Crane, B. R. *Biochemistry* **2002**, *41*, 11071−11079.